Dysregulation of miR-381-3p and miR-23b-3p in skeletal muscle could be a possible estimator of early post-mortem interval in rats

Vanessa Martínez-Rivera [1], **Christian A. Cárdenas-Monroy** [1], **Oliver Millan-Catalan** [2,3], **Jessica Gonzalez-Corona** [1], **Sofia Huerta-Pacheco** [4], **Antonio Martinez-Gutierrez** [2], **Alexa Villavicencio-Queijeiro** [1], **Carlos Pedraza-Lara** [5], **Alfredo Hidalgo-Miranda** [6], **María Elena Bravo-Gómez** [7], **Carlos Pérez-Plasencia** [2,3], **Mariano Guardado-Estrada** [Corresp. 1]

[1] Laboratorio de Genética de la Licenciatura en Ciencia Forense, Facultad de Medicina, Universidad Nacional Autónoma de México, Ciudad de México, Ciudad de México, México

[2] Laboratorio de Genómica, Instituo Nacional de Cancerologia, Ciudad de México, Ciudad de México, México

[3] Laboratorio de Genómica, Unidad de Biomedicina, Facultad de Estudios Superiores Iztacala, Universidad Nacional Autónoma de México, Ciudad de México, Ciudad de México, México

[4] Cátedras CONACYT - Ciencia Forense, Facultad de Medicina, Universidad Nacional Autónoma de México, Ciudad de México, Ciudad de México, México

[5] Laboratorio de Entomología de la Licenciatura en Ciencia Forense, Facultad de Medicina, Universidad Nacional Autónoma de México, Ciudad de México, Ciudad de México, México

[6] Laboratorio Genómica del Cáncer, Instituto Nacional de Medicina Genómica, Instituto Nacional de Medicina Genomica, Ciudad de México, Ciudad de México, México

[7] Laboratorio de Toxicología de la Licenciatura en Ciencia Forense, Facultad de Medicina, Universidad Nacional Autónoma de México, Ciudad de México, Ciudad de México, México

Corresponding Author: Mariano Guardado-Estrada
Email address: mguardado@cienciaforense.facmed.unam.mx

Background. The post-mortem interval (PMI) is defined as the time elapsed since the dead of an individual until the body is found, which is relevant for forensic purposes. The miRNAs regulate the expression of some genes and due to their small size, they can better support degradation, which makes them suitable for forensic purposes. In the present work we evaluated the gene expression of miR-381-3p, miR-23b-3p and miR-144-3p at the early PMI in skeletal muscle in a murine model.

Methods. We performed a rat model to evaluate the early PMI under controlled conditions. This model consisted in 25 rats divided into groups of five rats which correspond to the 0, 3, 6, 12 and 24 hours of PMI. Muscle tissue samples were taken from each rat to analyze the expression of miR-381-3p, miR-23b-3p and miR-144-3p by quantitative RT-PCR. The gene expression of each miRNA was calculated as *Fold Change* (FC) and compared among groups. To find the targets of these miRNAs and the pathways where they participate, we performed an in-silico analysis. Also, to evaluate if these miRNAs could predict the early PMI, a mixed effects model was calculated using their gene expression and the physical changes present in these rats.

Results. An up-regulation of miR-381-3p was found when we compared its gene expression between 0 and 24 h of PMI (FC= 1.02 vs. FC= 1.96; p=0.0079). This was the opposite for miR-23b-3p, which had a down-regulation at 24 h-PMI compared to 0 h-PMI (FC= 0.13 vs. FC= 1.22; p=0.0079). Moreover, the gene expression of miR-381-3p increased throughout the first 24 h of PMI, while it was the opposite for miR-23b-3p. The targets of these two miRNAs, participate in biological pathways related to hypoxia and RNA metabolism. Using a multivariate analysis, it was possible to predict the FC of miR-381-3p of all, but 6 h-PMI analyzed PMIs.

Discussion. The present results suggest that, miR-23b-3p and miR-381-3p participate at the early PMI probably regulating the expression of some genes related to the autolysis process. Although the miR-381-3p gene expression is a potential estimator of PMI, further studies will be required to confirm these results and obtain better estimates.

Dysregulation of miR-381-3p and miR-23b-3p in skeletal muscle could be a possible estimator of early post-mortem interval in rats.

Vanessa Martínez-Rivera[1], Christian A. Cárdenas-Monroy[1], Oliver Millan-Catalan[2,3], Jessica González-Corona[1], Sofia Huerta-Pacheco[4], Antonio Martinez-Gutierrez[2], Alexa Villavicencio-Queijeiro[1], Carlos Pedraza-Lara[6] , Alfredo Hidalgo-Miranda[5], María Elena Bravo-Gómez[7], Carlos Pérez-Plasencia[2,3], Mariano Guardado-Estrada[1]

[1] Laboratorio de Genética de la Licenciatura en Ciencia Forense, Facultad de Medicina, Universidad Nacional Autónoma de México, Ciudad de México, México.
[2] Laboratorio de Genómica, Instituto Nacional de Cancerología, Ciudad de México, México.
[3] Laboratorio de Genómica, Unidad de Biomedicina, Facultad de Estudios Superiores Iztacala, Universidad Nacional Autónoma de México, Estado de México, México.
[4] Cátedras CONACYT - Ciencia Forense, Facultad de Medicina, Universidad Nacional Autónoma de México, Ciudad de México, México.
[5] Laboratorio Genómica del Cáncer, Instituto Nacional de Medicina Genómica, Ciudad de México, México.
[6] Laboratorio de Entomología de la Licenciatura en Ciencia Forense, Facultad de Medicina, Universidad Nacional Autónoma de México, Ciudad de México, México.
[7] Laboratorio de Toxicología de la Licenciatura en Ciencia Forense, Facultad de Medicina, Universidad Nacional Autónoma de México, Ciudad de México, México.

Corresponding Author:
Mariano Guardado-Estrada[1]
Circuito de la Investigación SN, Ciudad Universitaria, C.P. 04360. Ciudad de México, UNAM. México. Email address: mguardado@cienciaforense.facmed.unam.mx

Abstract

Background. The post-mortem interval (PMI) is defined as the time elapsed since the dead of an individual until the body is found, which is relevant for forensic purposes. The miRNAs regulate the expression of some genes and due to their small size, they can better support degradation, which makes them suitable for forensic purposes. In the present work we evaluated the gene expression of miR-381-3p, miR-23b-3p and miR-144-3p at the early PMI in skeletal muscle in a murine model.

Methods. We performed a rat model to evaluate the early PMI under controlled conditions. This model consisted in 25 rats divided into groups of five rats which correspond to the 0, 3, 6, 12 and 24 hours of PMI. Muscle tissue samples were taken from each rat to analyze the expression of miR-381-3p, miR-23b-3p and miR-144-3p by quantitative RT-PCR. The gene expression of each miRNA was calculated as *Fold Change* (FC) and compared among groups. To find the targets of these miRNAs and the pathways where they participate, we performed an in-silico analysis. Also, to evaluate if these miRNAs could predict the early PMI, a mixed effects model was calculated using their gene expression and the physical changes present in these rats.

Results. An up-regulation of miR-381-3p was found when we compared its gene expression between 0 and 24 h of PMI (FC= 1.02 vs. FC= 1.96; p=0.0079). This was the opposite for miR-23b-3p, which had a down-regulation at 24 h-PMI compared to 0 h-PMI (FC= 0.13 vs. FC= 1.22; p=0.0079). Moreover, the gene expression of miR-381-3p increased throughout the first 24 h of PMI, while it was the opposite for miR-23b-3p. The targets of these two miRNAs, participate in biological pathways related to hypoxia and RNA metabolism. Using a multivariate analysis, it was possible to predict the FC of miR-381-3p of all, but 6 h-PMI analyzed PMIs.

Discussion. The present results suggest that, miR-23b-3p and miR-381-3p participate at the early PMI probably regulating the expression of some genes related to the autolysis process. Although the miR-381-3p gene expression is a potential estimator of PMI, further studies will be required to confirm these results and obtain better estimates.

Introduction

The post-mortem interval (PMI) is defined as the time elapsed since the dead of an individual, until the body is found, which is relevant for forensic purposes [1]. At early PMI (3 to 72 h after death), morphological changes appear, such as decay of temperature (algor mortis), cadaveric stiffness (rigors mortis) and changes in body coloration (livor mortis) [1,2]. The identification of these morphological changes is helpful to estimate the PMI. In the meantime, a process called autolysis occurs in the cells of a dead body, which is characterized by an absence of inflammatory response and a cell destruction due to liberation of the enzymes of some organelles [3].

However, the occurrence of these external morphological changes in a dead body, could vary due to different factors as the environment, cause of the death, among others, which could difficult to calculate accurately the PMI [4]. Thus, other methods have been developed, such as biochemical ones, in which some components in vitreous humor or synovial fluid are quantified for PMI estimation [4-8]. Nevertheless, as with physical changes, variations in factors affecting the quantifications of these elements reduce the confidence in the calculation of the PMI [4,9].

Other molecules that have been studied for PMI estimation are nucleic acids [10, 11]. For instance, it has been studied the RNA degradation in different tissues throughout the PMI [11]. Although it is expected that after the death of an individual the RNA transcription halts, there are many studies which analyze the expression of some genes at different PMI [12]. After the death, it has been found a transcriptional activity in different analyzed tissues of humans and other organisms [12, 13, 14]. For instance, in a study performed in mouse and zebra fish, it was found an upregulation of genes that participate in pathways as stress, immune response and apoptosis, among others [12]. In the case of humans, the changes of transcriptional activity at early PMI depend on the analyzed tissue, as well as with the rate of RNA degradation for each tissue [13]. Although there is not a fully explanation about the underlying mechanism of this transcriptional activity at PMI, it is suggested that epigenetic regulation could be involved, as histone modifications [12].

The miRNAs are small non-coding RNAs of a length of 22 nucleotides which can post-transcriptionally regulate the expression of genes implicated in several pathways [14]. Due to their small size, the miRNAs endure harsher conditions without degradation, which makes them suitable for forensic purposes [15, 16]. In fact, it has been reported that miRNAs regulate apoptosis, necrosis and autolysis, which are also implicated in the process of body decomposing [17-19]. Since miR-381-3p, miR-23b-3p and miR-144-3p participate in apoptosis and necrosis, in the present manuscript we analyzed their expression at early PMI in rat skeletal muscle. We established a PMI rat model to analyze, which allowed us to analyze the expression of these miRNAs in rat skeletal muscle according to the morphological changes present at early PMI. Finally, we evaluated whether the expression of these miRNAs could be used to estimate the PMI in these rats.

Materials & Methods

PMI rat model.

A total of 25 male Wistar rats were selected for the study, with an average weight of 200 gr. Rats were provided by the Faculty of Medicine's Animal House Academic Unit, from the National Autonomous University of Mexico (UNAM). In this Academic Unit the rats were housed in groups inside acrylic cages 20 cm height with floor area of 200 cm^2 per animal, without environmental enrichment because the social interaction is allowed. The controlled environmental conditions are temperature (22 ± 1 °C), 50–60% relative humidity, 12/12 h, light-darkness cycles. Animals were feed with Pellets Rodent 5001 (Lab Diet) and purified water *ad libitum*. These rats were euthanized by cervical dislocation as received in laboratory and sorted into five groups, which correspond to the 0, 3, 6, 12 and 24 hours of post-mortem interval (h-PMI). The 0 h-PMI was considered as the control group. The rats from 3, 6, 12 and 24 h-PMI groups, were euthanized by cervical dislocation and placed in a Binder KBW 240™ climatic chamber with a constant temperature of 25ºC. After the PMI time elapsed in each group, the presence of internal and external morphological changes was evaluated on every rat. Once the evaluation was performed, 200 mg of femoral muscle sample was obtained and stored at – 80ºC until analysis. Regarding to the control group, rats were euthanized, immediately analyzed, and the muscle sample taken thereafter. All procedures were evaluated and approved by the local ethic and scientific committee (approval number 102-2018), and the committee for the care and use of laboratory animals (CICUAL) with approval number 027-CIC-2018, of the Faculty of Medicine from the National Autonomous University of Mexico (UNAM). All animal procedures were performed strictly in accordance with local (NOM-062-ZOO-1999) and international norms of laboratory animals handling.

RNA extraction.

For miRNAs analysis, total RNA was extracted from the rat skeletal muscle samples using glass pearls for rupture and Trizol™ Reagent. In brief, a fraction between 50 and 100 mg of frozen tissue was collected in a 2 mL tube with 2 mm glass pearls (ZR BashingBead Lysis Tubes, Zymo Research) and 1 mL of Trizol™ Reagent. Then, 200 ul of clorophorm was added and mixed, to be centrifuged at 12, 000 g for 15 min at 4ºC. After this step, total RNA extraction was performed according to manufacturer's recommendations. RNA obtained was quantified with an UV- spectrophotomer NanoDrop™ 2000 (Thermo Scientific) and the integrity was evaluated qualitatively in agarose gels.

miRNAs quantification by RT-PCR.

From total RNA of muscle samples, miRNA cDNA was synthetized using the kit TaqMan Advanced miRNA cDNA Synthesis kit (Applied Biosystems). This kit performs the poly(A) tailing reaction and an adaptor ligation previously to the miRNA cDNA synthesis. All reactions were performed according to the manufacturer's protocol. Gene expression of miR-144-3p (rno481325_mir), miR-23b-3p (rno478602_mir) and miR-381-3p (rno481460_mir) were

evaluated with qRT-PCR using TaqMan® probes. The miR-361-5p (rno481127_mir) was used in as internal control, since it has been seen that its expression is stable under extreme conditions, such as cancer [20]. The miRNas quantification was performed in a StepOne™ Real-Time PCR System (Thermo Fisher Scientific, Waltham, Massachusetts, U.S.A) using 10 ng of total cDNA, 0.5 µl of the TaqMan® Advanced miRNA Assay (20X) and 5 µl of TaqMan® Fast Advanced Master Mix (2X) in a total volume of 7.5 µl. Each quantitative RT-PCR was incubated at 95°C for 20 s, then at 95°C for 3 min with 40 cycles of denaturation and annealing/extension at 60°C for 30 s. Each miRNA was analyzed separately and ran by triplicate in all samples. The average CT threshold calculated for each sample was used to relatively quantify the miR-144-3p, miR-23b-3p and miR-381-3p expression using the $2^{-\Delta\Delta CT}$ method expressed as Fold-Change (FC).

The miRNAs target identification analysis and their pathways.

The gene targets of the miRNAs miR-144-3p, miR-23b-3p and miR381-3p were identified in silico using several bioinformatic databases, which included predicted and experimentally validated targets. For predicted targets, the databases DIANA-microT-CDS [21,22], ElMMo (http://www.mirz.unibas.ch/ElMMo/), MicroCosm (https://omictools.com/microcosm-targets-tool), miRanda (http://www.microrna.org/microrna/getDownloads.do), miRDB (http://mirdb.org/), PicTar (https://pictar.mdc-berlin.de/), PITA (Segal Lab of Computational Biology, https://genie.weizmann.ac.il/pubs/mir07/mir07_prediction.html) and TargetScanHuman (http://www.targetscan.org/vert_72/) were used. On the other hand, the validated targets were searched in the miRecords (http://c1.accurascience.com/miRecords/), miRTarBase [23] and TarBase [24]. For each miRNA, it was selected those target genes which were present in at least three or more databases (Script in Supplemental Data 1). To identify the biological pathways were the miRNAs participate, these gene target list were further analyzed with the Gene Set Enrichment Analysis (GSEA) from WEB-based Gene SeT AnaLysis Toolkit (WebGestalt, http://www.webgestalt.org/). Only those biological pathways with a False Discovery Rate (FDR) less than 0.05 were considered.

Statistical analysis.

The FC of each miRNA was compared among the PMIs with the non-parametric Kruskal Wallis and the Mann U Whitney test. The presence or absence of morphological changes through the PMI in rats, were evaluated with the Multiple Correspondence Analysis. The dependence and association of the morphological changes with the PMI were evaluated with the Pearson's Chi-squared test and Cochran-Armitage test, respectively. A Mixed Effect Model was calculated considering the FC, the morphological changes of brain liquefaction and cerebral edema with PMI as independent variable ($y=X\beta+Z\gamma+\varepsilon$; where: y is the response vector of the all observations, X is a fixed effects design matrix, β is a p fixed effects vector, Z is a random effects design matrix, γ is a random effects vector and ε is the observation error vector). All

statistics were performed with the R-project software (https://www.r-project.org/). The dataset and scripts can be found in GitHub (https://github.com/nshuerta-ForenseUNAM/Dysregulation_miRNA).

Results

Morphological changes are heterogenous at different post-mortem intervals in rats.

Several internally and externally physical changes were evaluated at different post-mortem intervals in 25 rats. The externally physical changes evaluated included *algor mortis* (AM), *livor mortis* (LM), *rigor mortis* upper body (RMU), *rigor mortis* lower body (RML), drying (DR), generalized edema (ED), hair loss (HL), Abdomen green discoloration (AGD) and Abdominal distention (AD). All but RML, ED and AGD, appeared after the first 3 hours of PMI (see Table 1). On the other hand, the AGD was observed until the 12 h of PMI. In the case of *rigor mortis*, the RMU and the RML was only seen from 3 to 6 h-PMI and 6 to 12 h-PMI, respectively.

All animals were dissected to evaluate the following macroscopic characteristics: brain liquefaction (BL), brain edema (BE), discoloration of liver (DL), loss of liver consistency (LLC), muscle *livor mortis* (MML), bowel swelling (BS), ascites (AS) and loss of muscle consistency (LMC).

As the external characteristics, all these changes but AS and LMC, were gradually seen after 3 h of PMI. The only two characteristics that were present in all rats and in all PMI after 3 h of PMI, were DH and LML. The rest of the characteristics appeared gradually until they were fully present in all animals at 24 h-PMI. Interestingly, AS and LMC appeared until 24 h-PMI and they were present in the 60 and 80% of the analyzed animals, respectively.

These morphological changes were evaluated in a Multiple Correspondence Analysis (MCA), in order to see how these characteristics group through the analyzed PMIs (See Figure 1a). The MCA plot could capture at least the 74.2 % of the data and as it was expected, the morphological characteristics of the 0 h-PMI and the 24 h-PMI were located opposite to each other. Also, there were IPMs that clustered into three groups, because they shared some morphological characteristics among them (See Figure 1b). The first group included 0 and 3 h-PMI, the second the 6 and 12 h-PMI, and the third the 24 h-PMI. The group I is consistent with the few morphological changes present within the first 3 hour of PMI, while in the group III is where all the early PMI physical characteristics have been established. However, in the group II, there were characteristics which were present or absent in both, the 6 and 12 h-PMI, which not allowed to differentiate them in the MCA. These data suggest that the estimate of PMI using morphological changes could be more precise between 0 to 3 h-PMI and 24 h-PMI of death.

miR-381-3p and miR-23b-3p showed gene expression imbalances throughout different PMIs in rats

Gene expression of miR-381-3p, miR-23b-3p and miR-144-3p was analyzed with qRT-PCR in skeletal muscle of rats at the PMIs aforementioned (see Supplemental Data 2). Interestingly, the gene expression of miR-381-3p was upregulated at the 24 h-PMI group of rats compared with the 0 h-PMI control (FC= 1.02 vs. FC= 1.96; p=0.0079, Mann U Whitney test; Figure 2a). When the FC of miR-381-3p was analyzed through the different PMIs, the gene expression of this miRNA had a J-shape curve (see Figure 2a). First, within the three hours of PMI, the expression of miR-381-3p decreased from 1.02 to 0.73 and this difference was statistically significant (p=0.0317, Mann U Whitney test; Figure 2a). In fact, the difference in the miR-381-3p was more evident comparing the 3hr-IPM with the 24 h-IPM (p=0.0079, Mann U Whitney test). Nevertheless, after the 3 h-IPM, the expression of this miRNA gradually increased from 6 hours of PMI to 24 hour of PMI interval (see Figure 2a). As it was expected, the difference in the gene expression between 3 h-PMI and 12 h-PMI was statistically significant (p=0.032, Mann U Whitney test).

Contrary to miR-381-3p, the gene expression of miR-23b-3p decreased as the PMI increases to 24 hours. The gene expression of miR-23b-3p was downregulated at 24 h-PMI compared with 0 h-PMI, and this difference was statistically significant (FC= 1.22 vs. FC= 0.13; p=0.0079, Mann U Whitney test; Figure 2b). Interestingly, when the FC of miR-23b-3p was analyzed by the PMIs, the expression of this miRNA decreased from the 0 h-IPM to the 24 h-IPM (see Figure 2b). As with the 0 h-IPM, there were significant differences comparing 3 h-IPM vs 24 h-IPM (p=0.0079, Mann U Whitney test), 6 h-IPM vs. 24 h-IPM (p=0.0079, Mann U Whitney test) and 12 h-IPM vs. 24 h-IPM (p=0.0079, Mann U Whitney test).

Finally, although the FC of miR-114-3p decreased from 0 h-IPM to 6 h-IPM, these differences were not significant (p>0.05, Mann U Whitney test; see Figure 2c). In fact, the FC remained unchanged in the following two post-mortem intervals. These results suggest that there is a dysregulation in gene expression of miR-381-3p and miR- 23b-3p as the time of post-mortem interval increases in rats.

Biological process related to miR-381-3p and miR-23b-3p.

Using the bioinformatic tool WebGestalt (see material and methods) we identified the target genes of miR-381-3p and miR-23b-3p. A total of 2122 and 2076 genes were found to be regulated by miR-381-3p and miR-23b-3p, respectively (Supplemental Table 1). With each set of genes, a Gene Ontology enrichment analysis was performed to find the main biological process where they participate (see material and methods). In the case of miR-381-3p, a total of six biological process were found to be regulated by this miRNA (see Figure 3a). Interestingly four of these biological processes are related to RNA processing as transcription, synthesis and metabolism. The rest of the processes involved with this miRNA is the positive regulation of gene expression.

On the contrary, a total of nine biological processes were associated with miR-23b-3p, which were more heterogeneous compared with miR-381-3p (see Figure 3b). For instance, the two most enriched biological process were those related to hypoxia response and to oxygen levels. On the other hand, there were process related to development of central nervous system. Interestingly, other complex cellular pathways were implicated with this miRNA, as positive regulation of signaling, phosphorylation and cell location. Although none of the biological processes where this miRNA participated are related to apoptosis and inflammation, it seems that their function in IPM would be related to the decomposing process of the body.

Estimation of IPM analyzing gene expression of miR-381-3p.

A Spearman Rho correlation was calculated with the FC of miR-381-3p from 3 h-PMI to 24 h-PMI, showing a value of $r=1$ ($p=0.037$). In order to evaluate whether it is possible to estimate the FC according to IPM and morphological changes, a mixed effects model was calculated (see material and methods). From the morphological changes analyzed, only the presence of brain liquefaction and brain edema were significantly associated with the FC ($p < 0.01$). An approach to estimate the FC according to PMI of miR-381-3p was done with this model. First, the FC values respect to change of time (PMI) and the presence or absence of brain liquefaction and brain edema were estimated. Through this model, it is possible to indirectly calculate the PMI, comparing the real FC, with the calculated confidence interval of the estimated FC. The mean FC estimated for 0 h-PMI was 1.01 ± 0 (95% CI, 1.01-1.01), 3 h-PMI to 0.73 ± 0.04 (95% CI, 0.69- 0.77), 6 h-PMI to 1.26 ± 0.64 (95% CI, 0.62-1.90), 12 h-PMI to 1.47 ± 0 (95% CI, 1.47-1.47) and 24 h-PMI to 1.96 ± 0 (95% CI, 1.96-1.96) respectively. It is important that there is no variability in the PMIs of 0, 12 and 24 h, in the estimated values for the FC, so the value in both limits is the same as the mean. According to our results, although the FC of miR-381-3p could be a good predictor of the 0, 3, 12 and 24 h-PMI, the high variability observed at 6 h-PMI hinder the estimation of an accurate interval of PMI according to FC. Although the Spearman Rho correlation was negatively significant for the FC of miR-23b-3p according to IPM ($r = -0.9$, $p < 0.05$), there was not significance in the IPM and morphological variables when mixed effects model was calculated (data not shown).

Discussion

In the present work we found a gene expression dysregulation of miRNAs miR-381-3p and miR-23b-3p in skeletal muscle tissue of rats exposed at different post-mortem intervals. The miR-23b-3p gene expression decreased starting from 0 to 24 of PMI. On the contrary, the gene expression of miR-381-3p increased with a J-shape curve as the PMI increased. These two miRNAs regulate the expression of genes which participate in processes as hypoxia or oxygen depletion sensing, and RNA transcription. The Fold-change of miR-381-3p could be predicted according to the PMI, brain edema and brain liquefaction.

It has been previously described the presence of several miRNAs in various tissues, through the PMI in humans and in rats [25,26]. As expected, due to their small size, they can tolerate degradation since they can be found until late PMI [26]. However, the analyzed gene expression of some miRNAs has been mainly focused in finding control genes potentially useful for IPM calculation based on gene expression analysis in death bodies. For instance, the gene expression of miR-9 and miR-125b barely fluctuates throughout the different PMI analyzed in spleen [16]. Nevertheless, within the first 24 h of PMI, it has been found an increase or decrease of gene expression of some miRNAs [16]. In the rat's brain, it has been found that the gene expression of miR-16 slightly decreased from 0 to 24 h of PMI [27]. On the contrary, miR-124a, miR-205 and miR-21 increased their gene expression within the first 24 h of PMI in brain and skin [27, 28]. This suggest that the gene expression of miRNAs in dead bodies could be involved in the decomposing process, possibly regulating the expression of other genes, rather than being inert molecules which heavily resist degradation.

After the dead of an individual, the autolysis process is seen as a step necessary to achieve body decomposing and it occurs nearly immediately after the dead of the individual [29]. Nevertheless, more than the liberation of enzymes and proteasomal degradation, the autolysis process is a complex process in which a struggle between survival and pro-apoptotical signals takes place [30]. It is well known that there is a transcriptional activity of some genes in the PMI which could last for several days [13, 30, 31]. Thus, it is expected that those genes related to processes favoring the decomposing progression, as apoptosis, will be upregulated in the PMI [29]. On the other hand, it has been found that there is a decrease of gene expression of genes related to cell survival [31].

In the case of our study, although the expression of miR-381-3p diminished in the first three hours of PMI, it increased afterwards. In humans, the miR-381 has been considered as a tumor suppressor in prostate and non-small cell lung cancer inhibiting cell proliferation, invasion and migration through inhibition of nuclear factor-κB signaling [32,33]. Regarding the PMI, the increase of this miRNA expression could be as a mechanism for promoting apoptosis related to oxidative stress produced by the hypoxia. Another mechanism, where miR-381 could take part in PMI, is the inflammation inhibition in the autolysis process, since it has been that this miRNA also inhibits the inflammatory response [34].

Besides the biological process related with miR-381 mentioned above, this miRNA regulates genes related with biological pathways as RNA transcription and metabolism. Since these genes are targets of miR-381, it is expected that their expression could be downregulated. For instance, it has been found in several tissues that the *RNASE2* gene, which is a gene from the family of ribonucleases involved in RNA degradation, is downregulated as the PMI increased [13]. Also, at early PMI in skeletal muscle, it has been reported a decrease in the gene expression of genes related to processes like regulation of mRNA stability or poly(A) RNA binding [30]. This also suggest that miR-381 could be implicated in transcript stability regulation.

Contrary to miR-381, the miR-23b-3p showed a gradual reduction of its expression throughout the analyzed PMIs. The miR-23b-3p has been considered as an onco-miR in several types of

cancers, as gastric or breast cancer [35, 36]. In osteosarcoma, it has been found that miR-23b-3p promotes cell proliferation, while inhibits oxidative phosphorylation increasing the lactate levels in these cells [37]. However, it is important to emphasize that these results were found in in cancer, which could differ from PMI, where the metabolism of the cell is strictly anaerobic [38]. The proliferation mediated by miR-23b-3p is due to activation of TGF-β signaling by inhibition of *TGIF1* [39]. The results of the present study suggest that downregulation of miR-23b-3p that we found throughout the PMI, halts cell proliferation in cells of the dead body, at the start of the autolysis process. Also, miR-23b-3p regulates many genes which participate in process related to oxygen consumption. The downregulation of this miRNA suggests that it might be a corresponding response, at least within the first 24 h after the dead, of those response genes to lower levels of oxygen. For instance, it has been found in mouse, that in the first 24 h of PMI, there is an increase of hypoxia-related gene transcripts as *Degs2* [12]. The *Degs2* gene is an oxygen sensor which regulates cell-growth, death, angiogenesis, among other process [12]. In skeletal muscle and heart of humans, there is an upregulation of genes that participate in the oxidative phosphorylation and other mitochondrial protein synthesis [8]. Moreover, the gene expression of *HBA1*, which participate in oxygen transport, has been found to gradually increase in the early PMI [13]. This suggest that response to hypoxia seems is crucial in the PMI with glycolysis activation among other pathways, to desperately maintain the homeostasis.

Several works have used the C_T obtained from some genes to estimate the PMI through univariate or multivariate linear regression analysis with high coefficient of determination [16, 26, 40]. However, using the FC could be a better estimator of the relatively change of gene expression throughout the PMI respect with a control group. From the three miRNAs that we analyzed, the only significant model to estimate the FC was miR-381-3p with a good coefficient of determination (r^2= 0.91). However, these results should be taken cautiously due to the shape of the curve of miR-381-3p gene expression does not fit a linear model.

Although the mean FC of miR-381-3p was higher at 6 h-PMI compared with 0 and 3 h-PMI, this PMI presented also a high variability in the expression of this miRNA. This resulted in wide confidence intervals when the FC was estimated according to the PMI, which no allowed to accurately estimate at 6 h of PMI according to expression of this miRNA. The variation of gene expression of miR-381-3p at this PMI could be due to individual differences in the autolysis process at this PMI. Interestingly, these differences were also seen when the physical characteristics of the rats at different PMI were evaluated with the Multiple Correspondence Analysis. Thus, it is possible that the decomposing rate vary at 6 h of PMI resulting in rats which still present some characteristics of the immediate PMI, hindering its calculation.

Although we found differences in the gene expression of miR-381-3p and miR-23b-3p in rat skeletal muscle throughout the post-mortem interval, it is important to mention the limitations of the present study. The conditions of the experiments were performed in an animal model by controlling the environmental conditions, as temperature and humidity, which can differ drastically from real forensic scenarios. Thus, we cannot discard that the expression of these miRNAs could vary across different environmental conditions.

Conclusions

The gene expression dysregulation of miR-381-3p and miR-23b-3p found in rat muscle at early post-mortem interval, suggest that these miRNAs participate in the autolysis process. The dysregulation of these miRNAs could be related with alteration of the mRNA expression of some genes at early post-mortem interval reported in other studies. The targets of these miRNAs are involved in pathways related to hypoxia and RNA metabolism. Our results, with other reports, indicate that at early post-mortem interval, there is a transcriptional activity of several groups of genes. Although miR-381-3p gene expression could be a promising biomarker for post-mortem interval estimation, further studies will be required to refine these predictions.

Conflict of interests.

The authors have declared that there is not actual or potential conflict of interest in this work.

Acknowledgements

This study was part of the dissertation to obtain the Ms C. degree of Vanessa Martínez Rivera at the Posgrado de Maestría en Ciencias Biológicas, National Autonomous University of Mexico (UNAM).

Funding

This work was supported by the National Autonomous University of Mexico (UNAM), PAPIIT grant number **IA204420**. The funder had no role in study design, data collection and analysis, decision to publish, or preparation of the manuscript.

References

1. AE, Inoue CG, Barksdale LE, Carter DO. 2017. Toward a universal equation to estimate postmortem interval. Forensic Science International. 272:150-153. doi:10.1016/j.forsciint.2017.01.013
2. Lee Goff M. 2009. Early post-mortem changes and stages of decomposition in exposed cadavers. Experimental and Applied Acarology. 49(1-2):21-36. doi:10.1007/s10493-009-9284-9
3. Tomita Y, Nihira M, Ohno Y, Sato S. 2004. Ultrastructural changes during in situ early postmortem autolysis in kidney, pancreas, liver, heart and skeletal muscle of rats. Legal Med (Tokyo). 6(1):25-31. doi:10.1016/j.legalmed.2003.09.001
4. Madea B. 2016. Methods for determining time of death. Forensic Science, Medicine and Pathology. 12(4):451-485. doi:10.1007/s12024-016-9776-y
5. Zilg B, Bernard S, Alkass K, Berg S, Druid H. 2015. A new model for the estimation of time of death from vitreous potassium levels corrected for age and temperature. Forensic Science International. 254:158-166. doi:10.1016/j.forsciint.2015.07.020

6. Madea B, Käferstein H, Hermann N, Sticht G. 1994. Hypoxanthine in vitreous humor and cerebrospinal fluid--a marker of postmortem interval and prolonged (vital) hypoxia? Remarks also on hypoxanthine in SIDS. Forensic Science International. 65(1):19-31. doi:10.1016/0379-0738(94)90296-8
7. Ansari N, Menon SK. 2017. Determination of Time since Death using Vitreous Humor Tryptophan. Journal of Forensic Sciences. 62(5):1351-1356. doi:10.1111/1556-4029.13430
8. Madea B, Kreuser C, Banaschak S. 2001. Postmortem biochemical examination of synovial fluid--a preliminary study. Forensic Science International. 118(1):29-35. doi:10.1016/s0379-0738(00)00372-8
9. Muñoz Barús JI, Suárez-Peñaranda J, Otero XL, et al. 2002. Improved estimation of postmortem interval based on differential behaviour of vitreous potassium and hypoxantine in death by hanging. Forensic Science International. 125(1):67-74. doi:10.1016/s0379-0738(01)00616-8
10. Itani M, Yamamoto Y, Doi Y, Miyaishi S. 2011. Quantitative analysis of DNA degradation in the dead body. Acta Medica Okayama. 65(5):299-306. doi:10.18926/AMO/47011.
11. Koppelkamm A, Vennemann B, Lutz-Bonengel S, Fracasso T, Vennemann M. 2011. RNA integrity in post-mortem samples: influencing parameters and implications on RT-qPCR assays. International Journal of Legal Medicine.125(4):573-580. doi:10.1007/s00414-011-0578-1
12. Pozhitkov AE, Neme R, Domazet-Lošo T, et al. 2017. Tracing the dynamics of gene transcripts after organismal death. Open Biology. 7(1):160267. doi:10.1098/rsob.160267
13. Ferreira PG, Muñoz-Aguirre M, Reverter F, et al. 2018. The effects of death and post-mortem cold ischemia on human tissue transcriptomes. Nature Communications. 9(1):490. doi:10.1038/s41467-017-02772-x
14. Vishnoi A, Rani S. 2017. MiRNA Biogenesis and Regulation of Diseases: An Overview. Methods in Molecular Biology.1509:1-10. doi:10.1007/978-1-4939-6524-3_1
15. Hui Wang, Jiong Mao, Yingbi Li, et al. 2013. 5 miRNA expression analyze in post-mortem interval (PMI) within 48h. Forensic Science International: Genetics Supplement Series. 4(1):190-191. https://doi.org/10.1016/j.fsigss.2013.10.098.
16. Lv YH, Ma KJ, Zhang H, et al. 2014. A time course study demonstrating mRNA, microRNA, 18S rRNA, and U6 snRNA changes to estimate PMI in deceased rat's spleen. Journal of Forensic Sciences. 59(5):1286-1294. doi:10.1111/1556-4029.12447 3
17. Jiang X, Yu M, Zhu T, et al. 2020. Kcnq1ot1/miR-381-3p/ETS2 Axis Regulates Inflammation in Mouse Models of Acute Respiratory Distress Syndrome. Molecular Therapy — Nucleic Acids. 19:179-189. doi:10.1016/j.omtn.2019.10.036
18. Zhou W, Xu J, Wang C, Shi D, Yan Q. 2019. miR-23b-3p regulates apoptosis and autophagy via suppressing SIRT1 in lens epithelial cells. Journal of Cellular Biochemistry. 120(12):19635-19646. doi:10.1002/jcb.29270.

19. Chen G, Ma Y, Jiang Z, et al. 2018. Lico A Causes ER Stress and Apoptosis via Up-Regulating miR-144-3p in Human Lung Cancer Cell Line H292. Frontiers in Pharmacology. 9:837. doi:10.3389/fphar.2018.00837
20. Della Bella E, Stoddart MJ. 2019. Cell detachment rapidly induces changes in noncoding RNA expression in human mesenchymal stromal cells. Biotechniques. 67(6):286-293. doi:10.2144/btn-2019-0038
21. Paraskevopoulou MD, Georgakilas G, Kostoulas N, et al. 2013. DIANA-microT web server v5.0: service integration into miRNA functional analysis workflows. Nucleic Acids Research. 41:W169-W173. doi:10.1093/nar/gkt393
22. Reczko M, Maragkakis M, Alexiou P, Grosse I, Hatzigeorgiou AG. 2012. Functional microRNA targets in protein coding sequences. Bioinformatics. 28(6):771-776. doi:10.1093/bioinformatics/bts043
23. Chou CH, Shrestha S, Yang CD, et al. 2018. miRTarBase update 2018: a resource for experimentally validated microRNA-target interactions. Nucleic Acids Research. 246(D1):D296-D302. doi:10.1093/nar/gkx1067
24. Karagkouni D, Paraskevopoulou MD, Chatzopoulos S, et al. 2018. DIANA-TarBase v8: a decade-long collection of experimentally supported miRNA-gene interactions. Nucleic Acids Res. 46(D1):D239-D245. doi:10.1093/nar/gkx1141
25. Lv YH, Ma JL, Pan H, et al. 2017. Estimation of the human postmortem interval using an established rat mathematical model and multi-RNA markers. Forensic Science, Medicine and Pathology. 13(1):20-27. doi:10.1007/s12024-016-9827-4
26. Tu C, Du T, Ye X, Shao C, Xie J, Shen Y. 2019. Using miRNAs and circRNAs to estimate PMI in advanced stage. Legal Medicine (Tokyo). 38:51-57. doi:10.1016/j.legalmed.2019.04.002
27. Nagy C, Maheu M, Lopez JP, et al. 2015. Effects of postmortem interval on biomolecule integrity in the brain. Journal of Neuropathology & Experimental Neurology. 74(5):459-469. doi:10.1097/NEN.0000000000000190
28. Ibrahim, S.F., Ali, M.M., Basyouni, H. et al. 2019. Histological and miRNAs postmortem changes in incisional wound. Egyptian Journal of Forensic Sciences. 9(37):1-6 https://doi.org/10.1186/s41935-019-0141-7
29. Zapico S, Menéndez ST, Núñez P. 2014. Cell death proteins as markers of early postmortem interval. Cellular and Molecular Life Sciences. 71(15):2957-2962. doi:10.1007/s00018-013-1531-x
30. Sanoudou D, Kang PB, Haslett JN, Han M, Kunkel LM, Beggs AH. (2014) Transcriptional profile of postmortem skeletal muscle. Physiological Genomics. 16(2):222-228. doi:10.1152/physiolgenomics.00137.2003
31. Hu Y, Wang L, Yin Y, Yang E. 2017. Systematic analysis of gene expression patterns associated with postmortem interval in human tissues. Scientific Reports. 7(1):5435. doi:10.1038/s41598-017-05882-0

32. Formosa A, Markert EK, Lena AM, et al. 2014. MicroRNAs, miR-154, miR-299-5p, miR-376a, miR-376c, miR-377, miR-381, miR-487b, miR-485-3p, miR-495 and miR-654-3p, mapped to the 14q32.31 locus, regulate proliferation, apoptosis, migration and invasion in metastatic prostate cancer cells. Oncogene. 33(44):5173-5182. doi:10.1038/onc.2013.451

33. Huang RS, Zheng YL, Zhao J, Chun X. 2018. microRNA-381 suppresses the growth and increases cisplatin sensitivity in non-small cell lung cancer cells through inhibition of nuclear factor-κB signaling. Biomedicine & Pharmacotherapy. 98:538-544. doi:10.1016/j.biopha.2017.12.092

34. Chen WC, Luo J, Cao XQ, Cheng XG, He DW. 2018. Overexpression of miR-381-3p promotes the recovery of spinal cord injury. European Review for Medical and Pharmacological Sciences. 22(17):5429-5437. doi:10.26355/eurrev_201809_15802

35. Chen L, Han L, Zhang K, et al. 2012 VHL regulates the effects of miR-23b on glioma survival and invasion via suppression of HIF-1α/VEGF and β-catenin/Tcf-4 signaling. Neuro-Oncology. 14(8):1026-1036. doi:10.1093/neuonc/nos122

36. Hu X, Wang Y, Liang H, et al. 2017 miR-23a/b promote tumor growth and suppress apoptosis by targeting PDCD4 in gastric cancer. Cell Death and Disease. 8(10):e3059. Published 2017 Oct 5. doi:10.1038/cddis.2017.447

37. Zhu R, Li X, Ma Y. 2019. miR-23b-3p suppressing PGC1α promotes proliferation through reprogramming metabolism in osteosarcoma. Cell Death and Disease. 10(6):381. Published 2019 May 16. doi:10.1038/s41419-019-1614-1

38. Donaldson, A.E., Lamont, I.L. 2015. Metabolomics of post-mortem blood: identifying potential markers of post-mortem interval. Metabolomics 11:237–245. https://doi.org/10.1007/s11306-014-0691-5

39. Barbollat-Boutrand L, Joly-Tonetti N, Dos Santos M, et al. 2017. MicroRNA-23b-3p regulates human keratinocyte differentiation through repression of TGIF1 and activation of the TGF-ß-SMAD2 signaling pathway. Experimental Dermatology. 26(1):51-57. doi:10.1111/exd.13119

40. Li WC, Ma KJ, Lv YH, et al. 2014. Postmortem interval determination using 18S-rRNA and microRNA. Science & Justice Journal. 54(4):307-310. doi:10.1016/j.scijus.2014.03.001

Table 1(on next page)

Presence of the external and internal macroscopic morphological characteristics in rats at different post-mortem intervals.

Table 1. Presence of the external and internal macroscopic morphological characteristics in rats at different post-mortem intervals.

	Frequency %				
Morphological Changes	**0 h-PMI**	**3 h-PMI**	**6 h-PMI**	**12 h-PMI**	**24 h-PMI**
External					
Algor mortis (AM)	0	100	100	100	100
Livor mortis (LM)	0	100	100	100	100
Rigor mortis upper body (RMU)	0	100	100	0	0
Rigor mortis lower body (RML)	0	0	100	100	0
Drying (DR)	0	100	100	100	100
Generalized Edema (ED)	0	0	100	100	100
Hair loss (HL)	0	100	100	100	100
Abdomen green discoloration (AGD)	0	0	0	40	100
Abdominal distention (AD)	0	100	100	100	100
Internal					
Brain liquefaction (BL)	0	40	60	100	100
Brain edema (CE)	0	20	100	100	100
Discoloration of liver (DL)	0	60	80	100	100
Loss liver consistency (LLC)	0	20	60	80	100
Livor mortis muscle (LMM)	0	60	60	100	100
Bowel swelling (BS)	0	20	100	100	100
Ascites (AS)	0	0	0	0	60
Loss muscle consistency (LMC)	0	0	0	0	80

Figure 1

Multiple correspondence analysis (MCA) between the early post-mortem interval and the presence of morphological changes in rats.

A) MCA of the analyzed PMIs (0, 3, 6, 12 and 24 h) and the presence of internal and external morphological changes. **B)** MCA of the PMIs groups I (0 and 3 h), II (6 and 12 h) and III (24 h), and the presence of internal and external morphological changes. Both plots represented the greatest cumulative variability and could capture at least the 74.2 % of the data. Abbreviations of the morphological characteristics are shown in Table 1. Dots represent each rat, while squares are the dichotomic presence of morphological changes (0: absence, 1: presence). The dashed line ellipses shown the distribution of the rats throughout the PMI.

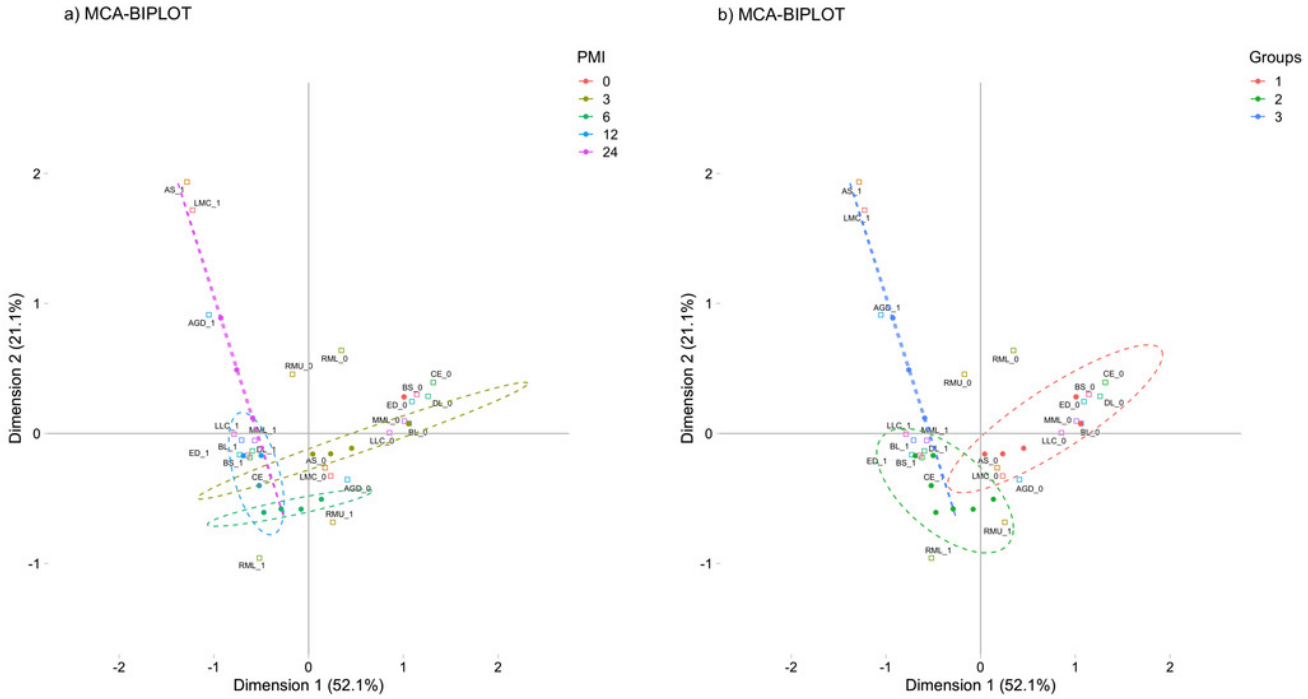
a) MCA-BIPLOT
PMI
0
3
6
12
24
Dimension 2 (21.1%)
Dimension 1 (52.1%)
b) MCA-BIPLOT
Groups
1
2
3
Dimension 2 (21.1%)
Dimension 1 (52.1%)

Figure 2

Gene expression analysis of miRNAs miR-381-3p, miR-23b-3p and miR-144-3p in rat skeletal muscle throughout the early different post-mortem interval.

The Fold-Change (FC) of miRNAs **A)**. miR-381-3p **B)**. miR-23b-3p and **C).** miR-144-3p was analyzed in rats skeletal muscle at 0, 3, 6, 12 and 24 hours of PMI using quantitative RT-qPCR. The Fold Change of each miRNA was calculated with the $2^{-\blacktriangle\blacktriangle CT}$ method using miR-361-5p as internal control. The black squares represent the mean of the FC from each group, the whisker corresponds to the 95% confidence interval and the dots are the jittered FC of each sample. Comparisons between the PMI were done with the Mann U- Whitney test. * p-value <0.05, ** p-value <0.01

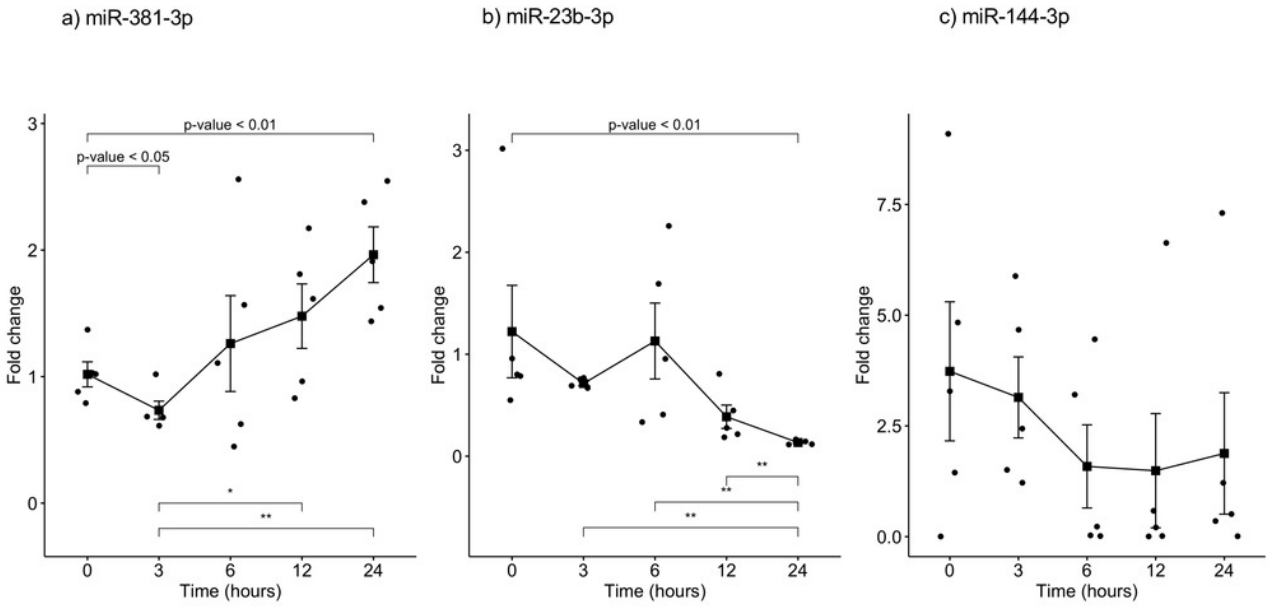
a) miR-381-3p
b) miR-23b-3p
c) miR-144-3p
p-value < 0.01
p-value < 0.05
Fold change
Time (hours)
0
3
6
12
24
*
**

Figure 3

Gene Ontology enrichment analysis.

The main biological pathways where the target genes of miRNAs **A)** miR- 381-3p and **B)** miR-23b-3p participate are shown. The *x*-axis correspond to the enrichment ratio and all the biological pathways have a False Discovery rate less than 0.05.